sciendo

TATRA MOUNTAINS
Mathematical Publications

DOI: 10.2478/tmmp-2020-0011
Tatra Mt. Math. Publ. **75** (2020), 163–190

ANALYSIS OF CELL DEATH BY IMAGE PROCESSING

Mária Ždímalová[1] — Tomáš Bohumel[1] —
Katarína Plachá-Gregorovská[2] —
Peter Weismann[3] — Hisham el Faloughy[3]

[1]Slovak University of Technology in Bratislava, SLOVAK REPUBLIC

[2]Institute of Experimental Pharmacology and Toxicology, Slovak Academy of Sciences, Bratislava, SLOVAK REPUBLIC

[3]Institute of Anatomy, Faculty of Medicine, Comenius University, Bratislava, SLOVAK REPUBLIC

ABSTRACT. In this paper, we present a graph theoretical approach to image processing with focus on the analysis of the biological data. We use the graph cut algorithms and extend them to obtain a segmentation of the biological cells. We introduce an utterly new algorithm for analysis of the resulting data and for sorting them into three main categories, which correspond to the biological cell death, based on the mathematical properties of the segmented elements.

1. Introduction

Graph theory has many real applications, e.g., in the economy, image processing [19], optimization problems, chemistry, etc.

We apply the graph theory to image processing. In computer vision, image segmentation is the process of dividing a digital image into multiple segments (sets of pixels, also called as super pixels). The objective of segmentation is to simplify or modify the representation of an image into something that is more significant and easier to analyse. Image segmentation is normally used to trace objects and boundaries (lines, dots, curves, etc.) that can occur in images.

2010 Mathematics Subject Classification: 92C73, 92C55, 94A08.
Keywords: graph cuts, segmentation, cell analysis, apoptosis, necrosis, computer morphometry.
This work was supported by the project of the Slovak Researcher and Development Agency, APVV-15-0205, APVV-14-0013, VEGA 1/0420/15.

Image processing and pre-processing are well-known and suitable tools for handling diverse types of data. In biology and medicine, the main aim is to simplify the representation of the obtained images for users. These methods are beneficial for handling medical and biological data as well. There are many approaches to image processing and pre-processing, e.g., trash-holding, graph cutting, level set methods and many others. We focus on the segmentation of objects, predominantly in our work on finding specific cells. In this concept, segmentation aims to distribute an image into regions and thus simplify its representation. Two types of regions are considered, namely object and background regions. The output of the segmentation is a binary image with extra information held representing "object" and "background" segments. We consider "objects" as all cells of interest and the "background" as the rest of the image. The primary goal of the segmentation is to simplify and change the representation of an image in the more meaningful and more accessible way for subsequent analyses. In our case, we deal with real biological data. We focus on the following analysis related to Parkinson's disease, Alzheimer's disease and amyotrophic lateral sclerosis which are significant neurological disorders of adults and are characterized by age-related neurodegeneration of many neural structures. Although in some forms of the mentioned disorders, hereditary factors play a role, the mechanism of cell death is not understood entirely.

The programmed cell death or the so-called apoptosis plays a role in many diseases, including heart diseases and cancer. It is also a vital cellular process that helps in regulation of tissue growth, foetal development, immune response and many other biological processes. A deviation from its precise control can lead to a number of disorders and health problems. Therefore, understanding the process of apoptosis is essential for the development of therapeutic approaches. Over the years, several procedures have been discovered and developed to detect it. There are several standard techniques such as electron microscopy, TUNEL assay, and flow cytometry. In addition, new techniques such as microfluidic devices, single-molecule spectroscopy, and electrochemical methods are emerging. From the very beginning of the study of apoptosis, it is known that cells at their advanced stages exhibit morphological changes characterized by nuclear and cytoplasmic condensation directing to fragmentation of cells into membrane-coated apoptotic bodies [13]. This can be observed by light microscopy, and their occurrence is subject to individual development. Initially, they are large fragments which then turn into numerous very small fragments [27]. Other morphological features of apoptosis occur in the absence of detectable DNA fragmentation or decrease of DNA content [5]. All of these findings can also be used in morphometric detection of apoptosis. Examination of cells by microscopy has been for a long time the basic technique for studying cellular function. When cells are appropriately stained, visual analysis can reveal a variety of biological mechanisms [4].

Like flow cytometry and image, cytometry is able to quantify the amount of protein or DNA. Moreover, it is also compatible with adherent cell cultures and can cope with time-laps samples. Also, image cytometry can accurately measure the structure and localization of proteins, as well as the shape and size of cells. Many researchers use the automated analysis of cells. Although there is no general, flexible software tool, several groups of researchers use automated cell analysis by creating custom scripts, macros, and plug-ins to meet specific image analysis tasks. Custom programs written in commercial software (such as MetaMorph, Image Pro Plus, MATLAB or Java) were many times used to identifying, measuring and monitoring cells in images and time records [15, 18, 25]. These studies demonstrate the power of automated image analysis for biological research. Moreover, the key challenges remain in the development of imaging analysis algorithms [20]. Cell culture imaging analysis has been described as one of the significant remaining challenges for screening [6, 7] and this area of research is lagging behind [17] the countless possibilities of imaging and analytical technologies currently [18]. It is difficult to replace the evaluation of image information by experienced professionals even with considerably sophisticated image analysis. While the expert evaluates only a few characteristics, image cytometry can extract a vast amount of information in detail characterizing the studied subject, which can greatly help to obtain relevant results in scientific research. One of these areas of research seems to be the detection of apoptosis/necrosis and their transient stages.

For a precise analysis of programmed cell death in neurodegenerative disease research, we have created a computer software to detect apoptosis/necrosis on histological preparations. We tested its functionality on histological preparations of brains gained from Wistar (7 days old), which we exposed to hypoxic-ischemic insult for 12 and 36 hours. We used coronal cryostat brain sections at the thickness of 30 micrometres, stained by cresyl violet. We tested pyramid cells in the region CA1 of the hippocampus. The brain of a rat P7 is histologically similar to a human embryo at 32–34 week of pregnancy. The aim of this work was an automated distinction, searching and the counting of specific cell types; the apoptotic, continuum of cell-death morphologies and necrotic cells, which are characterized below. Each of these three cellular categories has its particular features which are the size, the number of particle clusters from which these cells consist, the presence of cell wall and many others, see [14].

2. Graph theoretical approach to image processing

Methods based on the minimal cuts

In this part, we describe the methods based on a graph theoretical approach. However, at first we need to define certain concepts [3].

- Let $G = \big(V(G), E(G)\big)$ be a graph, where $V(G) = \{v_1, v_2, \ldots, v_n\}$ is the set of vertices that correspond to the image elements which might be represented as pixels or regions in Euclidean space. Let $E(G)$ be the set of edges that connect certain pairs of neighbouring vertices.
- Each edge $(v_i, v_j) \in E(G)$ is measured by the weight $w(v_i, v_j)$, which represents a certain quantity based on the property between the two vertices connected by that edge.
- The image can be divided into separate mutually exclusive components, being accepted that each component A is a connected graph

$$G = \big(V'(G), E'(G)\big), \quad \text{where} \quad V'(G) \subseteq V(G), \quad E'(G) \subseteq E(G)$$

  and $E'(G)$ contains only the edge of the vertices $V'(G)$.
- Therefore, the non-empty sets $A_1, A_2, \ldots, A_k$ form a division of the vertex set $V(G)$ if $A_i \cap A_j = \varnothing$ for $i \neq j, i$ and $j \in \{1, 2, \ldots, k\}$ and $A_1 \cup \ldots \cup A_k = V(G)$.
- For the components it should be valid that the properties such as the brightness value, colour and texture are similar throughout the whole component.
- Then, the degree of dissimilarity of two components can be calculated as the cut of the graph. A graph is related to a set of edges by which the graph G will be partitioned into two disjoint sets A and B.
- As a consequence, the segmentation of an image can be interpreted in the form of a graph cut. The graph cut value is defined as

$$cut(A, B) = \sum_{u \in A, v \in B(u,v)} w(u, v), \tag{1}$$

  where u and v are vertices of the different components. Afterwards, the issue of image segmentation can be treated as an optimization problem in which we try to minimize according to the certain criterion.
- In this case, it shall be optimal to divide the graph into two segments, which minimize the graph cut.
- The exact solution to image segmentation is hard to obtain. Therefore, it is more appropriate to solve this problem with the optimization method.
- The optimization-based approach formulates the problem as a minimization according to some established criterion, whereas one can find an exact or approximate solution to the original uncertain visual problem. The optimal bi-partitioning of a graph can be taken as the one which minimizes the cut value in the equation (1).

- Image segmentation can be formulated also as a labelling problem, where a set of labels L is assigned to a set of sites in S. In two class segmentation, for example problem can be described as assigning a label f_i from the set $\mathcal{L} = \{object, background\}$ to site $i \in S$, where the elements in S are the images or regions.
- Labelling can be performed separately from image partitioning. They achieve the same effort on image segmentation. Many methods perform both partitioning and labelling simultaneously [1, 19].

In the following text, we describe the basic partitioning methods using the knowledge from the graph theory [3].

Methods in image segmentation can be categorized into automatic methods and interactive methods. Automatic segmentation is desirable in many cases for its convenience and generality. However, in many applications such as medical or biomedical imaging, objects of intersect are often ill-defined so that even sophisticated automatic segmentation algorithms would fail. Interactive methods can improve the accuracy by incorporating prior knowledge from the user, however, in some practical applications where a large number of images are needed to be handled, they can be of high cost and much more time-consuming [10].

There are more methods from graph theoretical approach used in similar situations: minimal cuts, normalized graph cuts, graphs cuts with shape prior, interactive graph cuts methods, iterated graphs cuts, segmentation using minimal spanning trees, segmentation using Euler graphs and others. We focus on minimal graph cuts techniques.

3. Segmentation and Graph Cutting

The segmentation can be provided by many different techniques [12, 21]. The segmentation in the image processing can be formulated in mathematics as a minimization problem, see [11, 19]. Segmentation can work as a powerful energy minimization tool producing a globally optimal solution. For segmentation we use the mathematical method called "graph cutting", see [2,8,11]. In the present work, we have focused principally on Ford-Fulkerson and Edmonds-Karp algorithms [8, 9]. We process 2D image, which we first abstract as a graph (in a view of graph theory as a part of mathematics) and then we try to find a maximum flow in it. After finding the maximum flow [8], we can segment the image. The graph cuts are used in medical and biological image segmentation following few dynamic algorithms, finding the local minimum of the energy. Compared to the threshold technique, this approach gives more realistic results.

The principle of Ford-Fulkerson and Edmonds-Karp algorithms is based on increasing the flow in the graph (the network) through the augmenting paths. The algorithm progress while any augmenting path can be found. When there is no augmenting path available, the algorithm ends and the maximum flow is reached. The value of the maximum flow equals the sum of the capacities of the minimal cut edges.

The minimal cut is the result of the applied graph cut algorithms (mentioned above). The simplified explanation of finding the minimal cut is the process of pushing flow (imaginary units) from the source vertex named s to tank vertex named t through the graph consisting of the vertices and edges while possible. Once the process is finished and there is no capacity of the edges to transport any other flow, the minimal cut can be found as the union of such edges. In the image segmentation process, the pixels of any 2D image can be abstracted into the graph vertices and the graph used in the theoretical mathematics can be constructed.

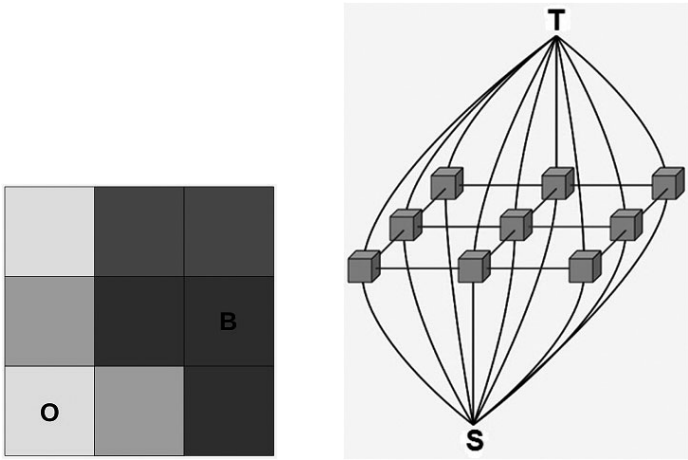

FIGURE 1. Left: Image with a background pixel and an object pixel. Right: Image transported to a network.

After that the graph cut algorithms can be applied, the minimal cut can be found, and finally, the image can be represented by the objects and the background. We process 2D image, which we first abstract as a graph and then we try to find a maximum flow in the obtained network, see Fig. 1.

After finding the maximum flow in network we can segment the image. The maximal flow in the network is equivalent to a minimal cut and it corresponds to segmentation, see Fig. 1, Fig. 2 and Fig. 3.

After that the graph cut algorithms can be applied, the minimal cut can be found, and finally, the image can be represented by the objects and the background.

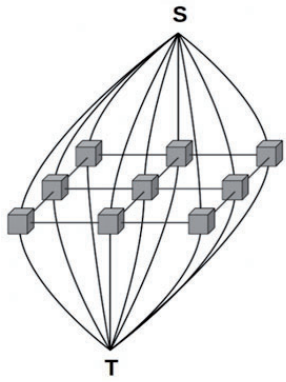

Pic. 7.1 a) Nonoriented graph

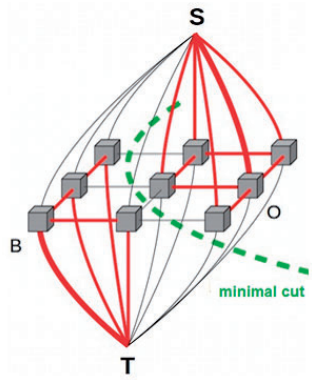

Pic. 7.1 b) Minimal cut

FIGURE 2. Left: Unoriented network. Right: Minimal cut.

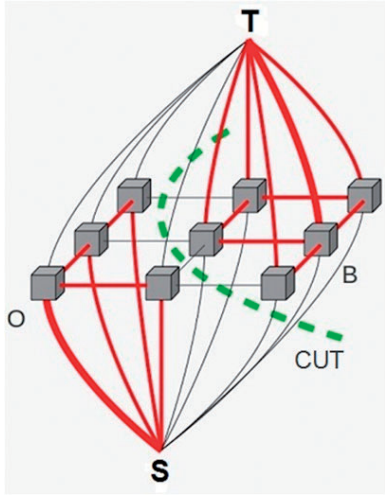

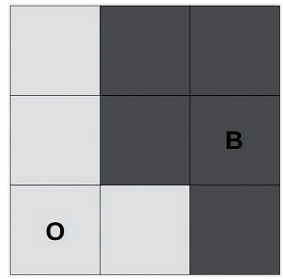

FIGURE 3. Left: Minimal cut. Right: Corresponding segmentation.

4. Program

For purposes mentioned in the above paragraph, we created the software with built in "graph cutting" algorithms for handling medical and biological data which are in our case output images from microscope. The advantage of this method is that it can provide global segmentation as well as local and we are also able to detect the edges, which represent the boundaries between cells. In our specific case we need to provide the pre-processing of the images as well. We apply the Gaussian kernel for pre-processing of the first input data from electronic microscope. The main benefit of this software is its complexity. It is able to do pre-processing of the images, segmentation of the image, which in our special case means finding the corresponding cells, and finally counting and categorize the cells. Once the process of the image segmentation, cell counting and categorization is done, the user can manually adjust image output (change the categories of marked cells, etc.) and use numerical output for the statistics.

The process of the image segmentation and cell categorization consists of the following steps:

(1) Data gathering from the microscope.

(2) Pre-processing of the data.

(3) Software initialization and specific input image loading.

(4) Setting up the object and background pixels of the image.

(5) Image segmentation process.

(6) Setting up the parameters for each of the cell types.

(7) Counting, colour marking and categorization of the cell types.

(8) Manual adjustment of the marked cells done by user.

(9) Output saving (image and numerical data).

The application of the image segmentation described above is used to identify three different types of cells presented in the images produced by the microscope which are the apoptosis, the nuclear morphology and the necrosis. Once the segmentation is done, we have to differentiate the segmented objects and group them together, because each of the cell types consists of many smaller objects. Each group of the segmented objects consists of the objects that have characteristic sizes, distances between each other and quantities due to what they can be categorized as one of the three cell categories.

5. Application in biological data

5.1. Materials and methods

5.1.1. Ethics

All procedures involving the animals were performed in compliance with the Principles of Laboratory Animal Care issued by the Ethical Committee of the Institute of Experimental Pharmacology and Toxicology, Slovak Academy of Sciences and by the State Veterinary and Food Administration of Slovakia. Adult Wistar rats were used from the breeding station Dobra Voda (Slovak Republic, reg. No. SK CH 24011). The rats had free access to water and food pellets and were kept under controlled conditions at 22° C and 12 h light/dark cycle. After seven days of adaptation, the females were mated with males in the ratio 3:1 for five days. Females were allowed to give birth in the term and the litters were culled within 24 h of birth to ten pups per litter (total 80 rat male pups).

5.1.2. Animals

Seven days old males pups (weight 13 –18 g) were subjected to the HI procedure according to modifications. The pups were anesthetized with isoflurane (Isoflurane or Forane, 4 percent induction and 2 percent for maintenance) and the duration of anaesthesia was less than 10 minutes. The left common carotid artery was isolated from the vagus nerve and jugular vein and permanently occluded with surgical silk and the incision was then closed. The pups were let to recover with their respective dams for 1 hour. Subsequently, they were separated from their mothers and placed in a temperature-controlled incubator (by Testo 310 residential combustion analyser) set to an ambient temperature 34° C and were exposed to 90 minutes of hypoxia (air atmosphere with 8 percent oxygen and abundant nitrogen). Afterwards, the pups were returned to the dams until sacrifice. Sham controls were submitted to anaesthesia and the neck incision without artery occlusion and were placed in a temperature-controlled incubator set to an ambient temperature of 34° C. Our profile of neuronal cell death could be different from other authors used the RV model with $36° - 37°$ C in a hypoxic chamber. We did not use 37° C in the hypoxic chamber as in original of the RV model for frequent loss of tissue in CA1 region what could thwart our cells counting method.

5.1.3. Tissue preparation

Tissue preparation. The pups were rapidly decapitated immediately after the hypoxia (0 h after the HII) or were sacrificed at various time periods

$$(1, 3, 12, 24, 36, 48, 72, 144, 192).$$

Brains were quickly removed to a 4 % paraformaldehyde (PFA). There were six males per group after the HII, four males in shames.

Results were first obtained by microscope (Olympus BX51). However, for automatic handling with a significant number of data we created software for automatic segmentation. Some data were first pre-processed on the microscope (Olympus BX51, see Fig. 4 and Fig. 5) or by own methods. We illustrate results obtaining by microscopy and just "handy" marking of the corresponding cells.

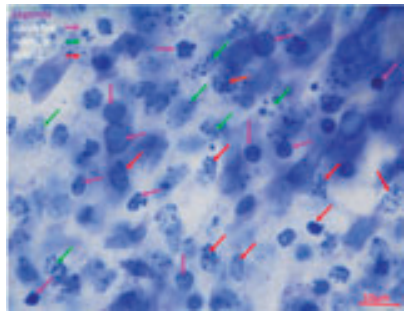

FIGURE 4. Damaged neurons in CA1 at 24 h after HII. Olympus BX51, magnification 60x, illustrated photo (our experiment). Apoptosis refers to pink, green necrosis and hybrid red arrows. Unintentional neurons are not present, as illustrated by a photo.

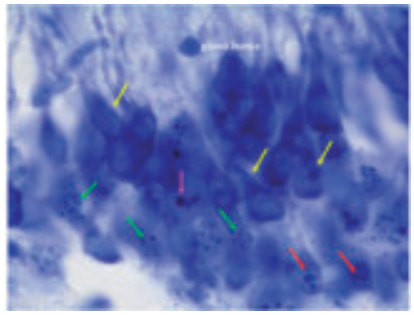

FIGURE 5. Phenotypes of cell death in CA1 at 24 h after HII. Olympus BX51, magnification 100x, illustrates a photo (our experiment). Apoptosis refers to pink, green necrosis, hybrid red and undamaged yellow arrows. Described is a glial cell, illustrated by a photo.

The coronal sections were visualized using a light microscope (Olympus BX51) and were photographed with camera (Olympus XM10, U-TV1X-2) and image analysis software (Cell-P, Olympus).

We created a program processing these data.
First, we show the input data, see Fig. 6.

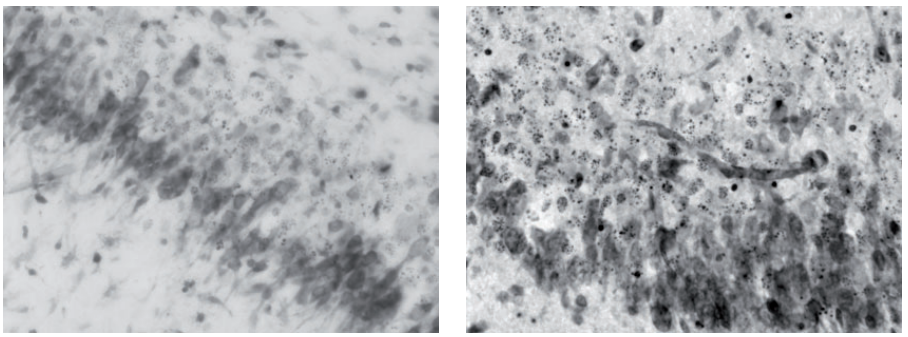

FIGURE 6. Examples of input data from microscope.

5.1.4. Computer process

The whole process of dealing with data (images) consists of three main steps: pre-processing of obtained data, processing and post-processing of data. Pre--processing is devoted to the correction and the preparation of data obtained from the microscope. Under the processing of data, we understand handling with the data from a graph theoretical approach. The last step is devoted to the final analyses of resulting data.

a) Pre-processing

Pre–processing is the whole preparation of the data before segmentation. Our input data are medical images from microscope, which are necessary to transform to 24 bit map and afterwards to correct contrast of input data whose purpose is that the resulting images are not too dark or too light and with well visible contours. We use two methods, the normalization of the histogram and the shading corrections.

Normalization of the histogram

Input data (microscope images) are taken by professional microscope with certain intensities. The range of intensities of the microscope are multiple times bigger, as we usual work in image processing (265 of values). Images in unusual format obtained in such a way that they have low contrast. It means that in histogram the values are cumulated on a small interval (scaling problem).

Normalization of the histogram corrects the distribution of intensities, and so it changes their range and, in this way, it improves the contrast of the image. The next linear transformation transforms values of intensities of pixels $\langle L, U\rangle$ for new values I_{new} from the interval in range $\langle L_{\text{new}}, U_{\text{new}}\rangle$.

$$I_{\text{new}} = (I_p - L)\frac{U_{\text{new}} - L_{\text{new}}}{U - L} + L_{\text{new}}.$$

The method mentioned above fails in case when in interval $\langle L, U\rangle$ appears only one pixel with a very small or very high intensity, which exceeds the top of interval of the histogram, and hence it is outside the range of intensities of pixels I_p creating the ratio in the histogram (image). In such a case, the intervals $\langle L, U\rangle$ and $\langle L_{\text{new}}, U_{\text{new}}\rangle$ are almost identified and the requested effect is not reached.

It is more reliable to choose some percentile of the original histogram for L and U. The range of the interval $\langle L, U\rangle$ will be 90 % of pixels of the origin range cumulated around the top of the histogram.

Shading correction

The shading correction is a background correction in an image meant to compensate for irregular illumination effects. This correction is also known as unsharp masking. In our work, we use it for increasing the difference between "background" and "object".

b) Processing

In this part, all graph algorithms are implemented in the segmentation of image. The pre-processing and correction soft input data of requested quality follows their processing. We normalize the images by the histogram and the shading corrections. The output S are segmented data, which are classified in other process.

For searching the maximal flow of the network, we use the Edmonds-Karp algorithm. We have implemented the algorithm with minor variations in comparison to the original one. For segmentation, we use and extend the method of graph cutting, see the Sections 5, 6, [2] and [16, 23]. We modify some steps of algorithm and optimize the fast run of the algorithm.

The result of the segmentation (processing) is the image classified into two classes: object and background pixels. The fact and information, if the resulting pixel belongs after segmentation to the background or the object is important by post analysis (post-processing). Post-processing is devoted to classifying the obtained cells. Since we need to distinguish concrete types of cells, it is necessary to create a new algorithm to classify obtained cells.

c) Post-processing: Characterization of output data — New algorithm for classification of cells

After finishing the segmentation we use the segmented image for the next analysis — the distinguishing, searching and the counting of concrete types of cells. We focus particularly on distinguishing the cells according to their death. In our work we consider three specific categories:

(1) the apoptosis (apoptotic cells),

(2) the nuclear morphology (hybrid cells),

(3) the necrosis (necrotic cells).

From the mathematical and programming point of view, we do not distinguish categories of the cells according the type of death. We need to use characteristics which are recognizable by analysing of image, which are objectively described by properties of the corresponding categories. It means categories which we are able to measure. Every category has its typical mathematical properties.

Apoptosis

From medical point of view, the apoptosis is a regulated death of the cell on the polycells organism. The cell simply die (or necrosis), after that they create big clumps of cells, which concentrate to some of larger whole (mostly of 1–3 pieces). In this process, the cell wall does not break down.

From the mathematical point of view, the apoptosis is characterized by a group of objects, which consists of the bigger number of pixels. The average value of distances of the centres of objects is approximately equal to the average value of one and a half times the of the sum the radii of all couples of objects, see Fig. 7.

The continuum of cell-death morphology

The nuclear morphology is the intermediate state between the apoptosis and the necrosis, called as well apoptosis-necrosis continuum. Larger wholes which arise by apoptosis will be finally decomposed. However, they are still markedly many times larger than by necroses. The wall of the cell remains without any break points.

The nuclear morphology (the hybrid state) is, in the sense of image processing, the group of more objects of multiple fewer proportions than there are proportions of objects creating apoptosis. These are in a distance approximately twice as large as is the distance of radii of two objects of any objects, as it is shown in Fig. 8.

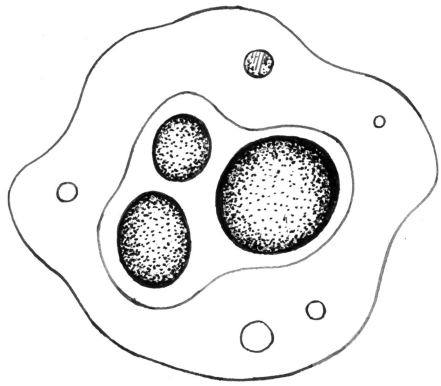

FIGURE 7. Image of the apoptosis.

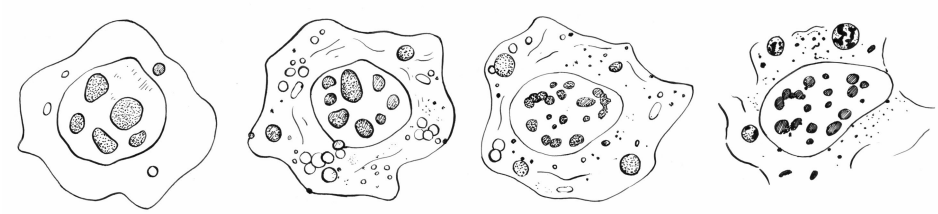

FIGURE 8. Image of the nuclear morphology.

Necrosis

By the definition, necrosis is a form of traumatic cell death. This type of death is conditioned by acute injury or damage the cell. The death occurs by breaking down the cell wall, which eventually almost completely disappears, and the inside of the cell (the clump of particles) dissolves into the space. These elements are then smaller, but they form larger aggregates.

From the point of view of the image analysis, the necrosis, see Fig. 9, is represented by miniature objects with dimensions that are several times smaller than the distances between these objects compared to the apoptosis and the morphology.

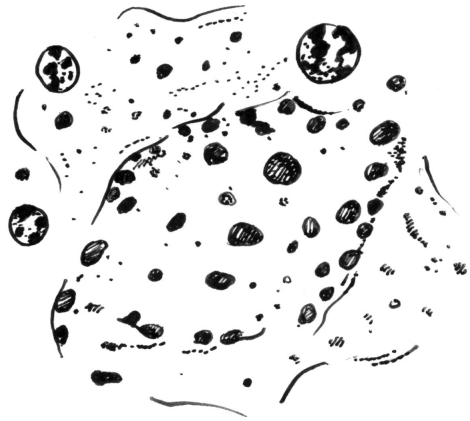

FIGURE 9. The image of the Necrosis.

Algorithm for Analysing Types of Cells

As we mentioned before, we created a new algorithm for analysing of cells. It is able to make the categorization of segmented cells and to sum them. It consists of steps described bellow.

Detection of objects is a process where we check the whole image and count the number of pixels, which were denoted by segmentation as the object pixels. We enumerate every object pixel by a number, see Fig. 10 left.

Enumerating of objects goes this way: we check the whole image again and all numbered pixels are assigned to certainly objects, which are subsequently enumerated. The results are the enumerated objects (families of objected pixels) as shown in Fig. 10 right.

Measuring the size of objects we obtain by summing up of all pixels, which appear in the corresponding enumerated object. The size of the object is given by the number of pixels and it is one of the criteria needed for categorization of the cells, see Fig. 11 left.

Classification of objects according to the size is made in such a way that we consider all objects (elements) which possess with typical size for given category of the cell. We just ignore all other objects.

Re-numbering is achieved by checking again all enumerated objects. Those ignored in the previous step are not enumerated. In this step, we select all objects which will be used by categorization of cells.

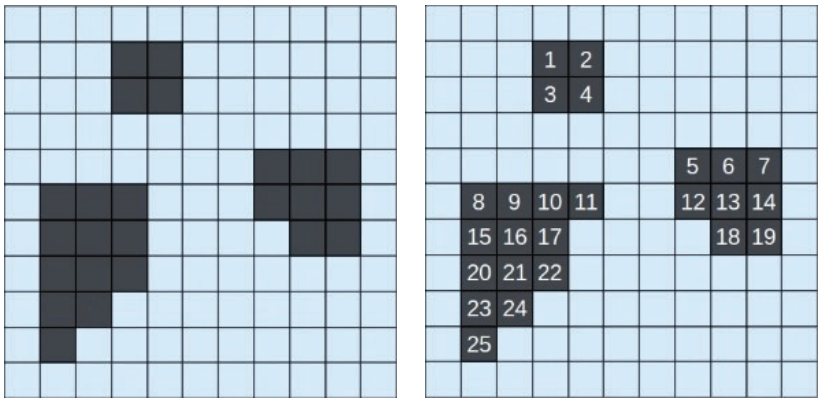

FIGURE 10. Left: Detection of the cells. Right: Enumerating of the objects.

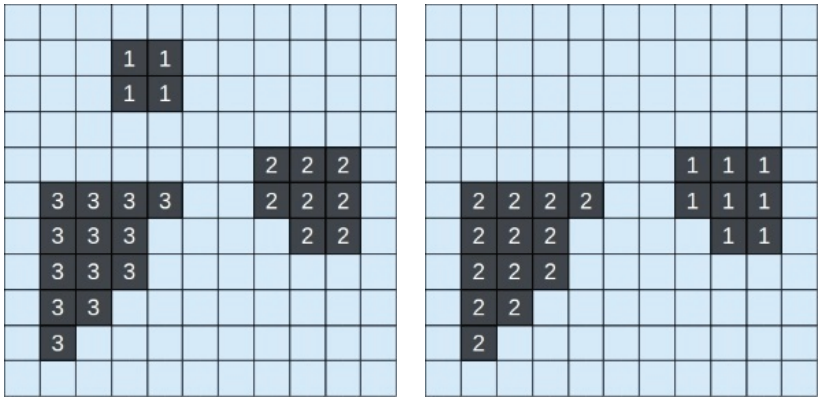

FIGURE 11. Left: Measuring of cells. Right: Re-numbering of objects.

Detection of the middle pixels of cells. It is possible to find the middle enumerated pixels of objects by recognizing its coordinates for each pixel that is a part of the numbered object. We calculate the value of the mean pixel as the arithmetic mean of pixel coordinates that belong to that concrete enumerated objects, as it is shown in Fig. 11 right.

Object distance measurement is the step in which we compare distances (in pixels) between the mean pixels of enumerated objects (elements) which are by their size typical for a given cell category. If the average pixels of the objects are in some special distance typically for a certain cell category then the clusters of these objects will create specific cells, see Fig. 12 left.

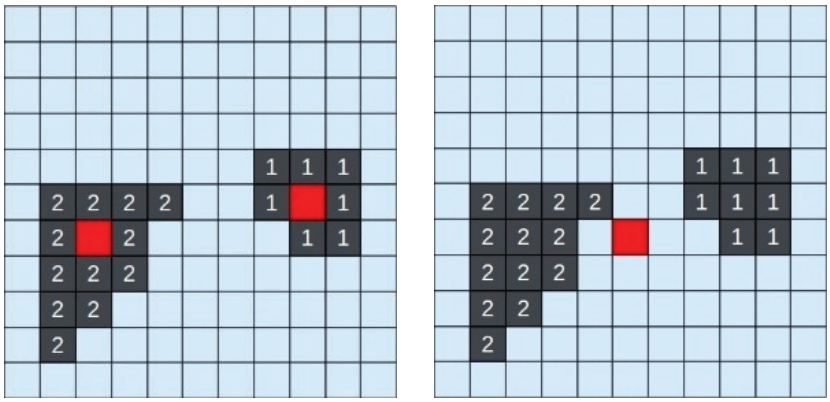

FIGURE 12. Left: Measuring the distances of objects, Right: Detection of the middle pixel of the cell.

Determination of the mean pixels of the cells is achieved by finding a mean pixel for each concrete cluster-aggregate. That means that the middle pixel of the objects is that of acceptable size and at the acceptable distances. Then we calculate the average pixel value of a particular cell as the arithmetic average of the coordinates of the middle pixels of the objects in the given particle cluster of elements, see Fig. 12 right.

Counting and summing up of the cells is the last step in which we can easily calculate the middle pixels of a given cell category, that is, the number of middle pixels of apoptotic, hybrid and necrotic cells.

6. Implementation in the program

We describe the implementation of the graph theory approach in the creation of a program to obtain the segmentation. The program is written in the language C. For searching of maximal flow of the network we used the Edmonds--Karp algorithm. We modified some steps of the algorithm, and we did optimization of the fast running of the algorithm. We decreased mainly the number of iterations. Finally, if the number of iterations was not possible to decrease, we decreased the number of operations, which were done in this iteration, to the minimum. The program consists of three main parts. The first one is the initialization, which describes and specifies our approach to the network. Another part is the algorithm for finding of maximal flow of the network. The last step is the processing of the resulting segmented data.

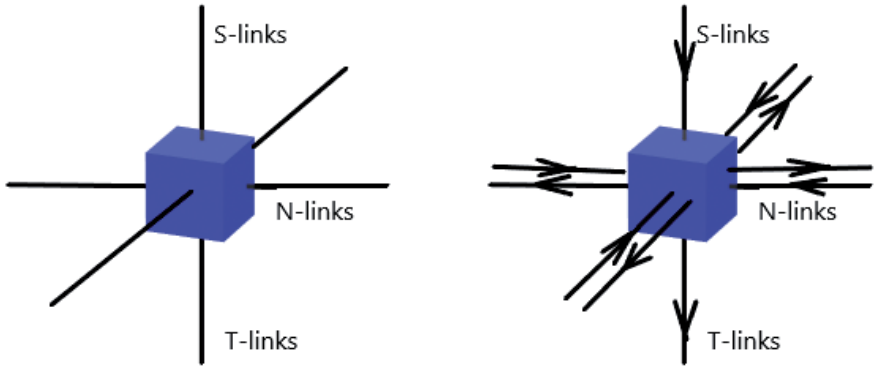

FIGURE 13. N-links and T-links [16].

Capacity of the Edges

We count the capacity for the corresponding links (edges). That one, which connects precisely two of neighbouring pixels (vertices) p and q we call N-links. That links, which connect precisely one pixel with the source s and the sink t, we call T-links, where the pixel is presented as a grey cube, see Fig. 13, N-links as horizontal links, and T-links as vertical lines. For more information about the implementation and the transformation to the network, see [23]. We use the following notation for the counting of the capacities:

P : the set of all pixels,

(p, q) : the edge connecting neighbouring pixels p and q,

I_p : the value of the intensity of the pixel p,

M : the maximal value of the intensity of the pixel (of the respective figure),

D : the difference of the maximal and minimal value of the intensity of the pixel (of the respective figure),

O_{avr} : the average value of the respective intensity of object seed pixels,

B_{avr} : the average value of the intensity of the background seed pixels,

$S(p)$: the capacity of the edge (link) connecting the sink (the vertex s) and corresponding pixel p,

$T(p)$: the capacity of the edge (link) connected output source (the vertex t) and concrete pixel (the vertex p),

$N(p, q)$: the capacity of the edge (link) connected neighbours pixels p a q,

λ : the weighing constant.

The weighing constant λ determines the result of the segmentation. The note $N(p,q)$ express the relationship between intensities of p and q, $S(p)$ and $T(p)$ express the relationship between intensity values of pixels and the values O_{avr} and B_{avr}, see Table 6. More details about the connection between these variables and constants can be found in [16, 23].

TABLE 1. The capacity evaluation.

Type	**Edge**	**Capacity**	
N-links	(p,q)	if $(p,q) \in P$	$N(p,q)$
T-links	(s,p)	if $p \in P \setminus \{o \cup B\}$	$\lambda S(p)$
		if $p \in O$	0
		if $p \in B$	0
S-links	(p,t)	if $p \in P \setminus \{o \cup B\}$	$\lambda T(p)$
		if $p \in O$	0
		if $p \in B$	∞

Capacity Evaluation

First, we select the values $S(p)$ and $T(p)$ for pixels p, which we have denoted as object seed pixels and background seed pixels. The value $S(p)$ will have the value of infinity, when we denoted the pixel p as object seed pixel, so $S(p) = \infty$. It is because $S(p)$ can never be saturated, since it connects the source s and object pixel. It means that object pixel need to be always reachable from the source s. The note $T(p)$ will have the value 0, when we denoted the pixel p as object seed pixel, so $T(p) = 0$. It is because this edge needs to be saturated and output t should not be reachable from the pixel p. Similarly, but vice versa, we do similar assignments also for all background seed pixels. We guarantee this way that after finishing the process the object seed pixels will surely be the part of the object and background seed pixels will be part of the background.

Linear Diffusion Coefficient

Capacities of N-links and T-links depend on intensities of the particular pixel. Other values of capacities, we count from the values of intensities of pixels as follows: Both N-line and T-line capacities depend on the intensity of the pixel.

Therefore, the next capacity values are calculated from the pixel intensity values as follows [16]:

$$\begin{aligned} N(p,q) &= D - |I_p - I_q|\,, \\ S(p) &= M - |O_{avr} - I_p|\,, \\ T(p) &= M - |B_{avr} - I_p|\,. \end{aligned}$$

It is precise because of the character (definition) of the M and D constants that the capacities are played non-negative. In extreme cases, some capacities may be zero. Considering all previous claims, we assign specific capacities to specific edges in the way as shown in Table 6.

Non-linear Diffusion Coefficient

We suggest a new different approach on how to give values to edges as well. If we want to approach the assignment of N-line capacities in a way that takes greater account of the relative intensity of pixel intensities and penalizes their differences, it is necessary to choose a non-linear coefficient for calculating their capacity. The non-linear coefficient causes neighbouring pixels with similar intensity values to have high-capacity edges (lines) and a certain drop in intensity of the neighbouring pixels, and the edge-to-edge gain is almost zero. For the interpretation of the next formulas the following definition is needed:

- s – absolute value of intensity difference of two neighbouring pixels,
- σ – penalizing constant,
- k – the penalty.

Thus, the value s is calculated as the absolute value of the difference between two adjacent pixels in the picture, the penalizing constant σ is optional and affects the course of functions, especially how rapidly their first derivation changes and the penalty k is given by the formula $k = \sigma^2$.

TV diffusion coefficient

$$d(s) = \frac{1}{s}, \qquad s \in N\,;$$

BFB diffusion coefficient

$$d(s) = \frac{1}{s^2}, \qquad s \in N\,;$$

Charbonnier diffusion coefficient

$$d(s) = \frac{1}{\sqrt{(1 + \frac{s^2}{k^2})}}, \qquad s \in N\,;$$

Perona-Malik diffusion coefficient

$$d(s) = \frac{1}{1 + (\frac{s}{k})^2}, \qquad s \in N\,;$$

$$d(s) = e^{-(\frac{s}{k})^2}, \qquad s \in N\,.$$

Weickert diffusion coefficient

$$d(s) = \left\{ \begin{array}{cc} 1 & s = 0 \\ 1 - e^{\frac{-3.31488}{(s/K)^8}} & s > 0 \end{array} \right\}, \quad s \in \mathbb{N}\,.$$

Comparison of diffusion coefficients

The diagram in Fig. 14 shows the comparison of diffusion coefficients which depend on the intensity differences from 0,255 at the selected value as follows:

- Linear coefficient - blue,
- TV coefficient - red,
- BFB coefficient - purple,
- Charbonnier coefficient - yellow,
- Perona-Malik coefficient - green and - black,
- Weickert coefficient - orange.

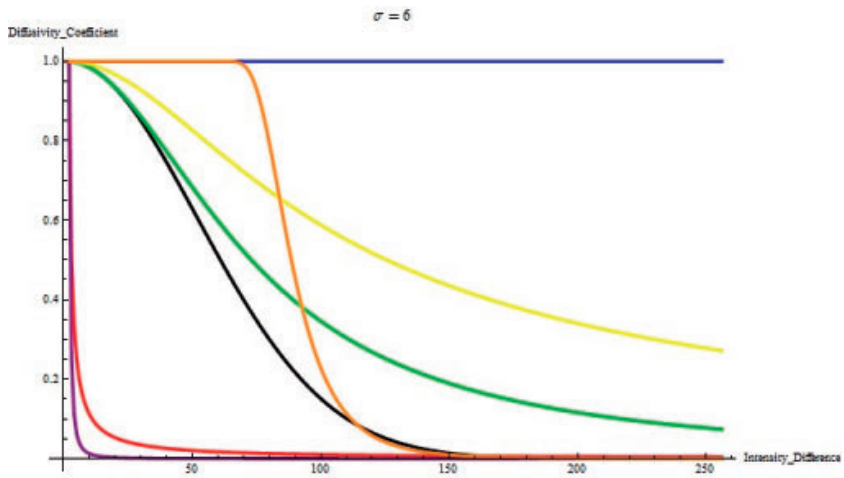

FIGURE 14. Comparision of diffusion coefficients.

Using different types of coefficients help us to obtain better segmentation and better results. From the programming point of view, the implementation can be divided into three main parts, which can also be further elaborated, namely marked. They are as follows: marking procedure, path reconstruction and the distribution of vertices.

The whole program is available on `http://www.math.sk/wiki/zdimalova` in Section : Project

: Graph theory approach to image processing

: Common work with Tomas Bohumel, Weisman Peter, El Faloughy Hisham

: Cell analysis Program segmentation : segmentation 1,
segmentation 2,
segmentation 3,
segmentation 4.

7. Results

We have used the application of the image segmentation to identify three different types of cells presented in the images observed and gained by the light microscope. They are the apoptosis, the continuum of cell-death morphologies and the necrosis. When we finished the segmentation, see Figure 15, we were able to differentiate segmented objects and group them. Each of the cell types consisted of many smaller pieces like objects. Each of these segmented objects consisted of another objects which had the corresponding sizes, distances between each other and quantities because they could be categorized into three main categories. Below, there is a part of the input and the output image, Figure 16, with marked apoptosis (red), the continuum of cell-death morphologies (blue) and necrosis (green). Figures 17, 18, 19, 20 show the input samples, the samples after pre-processing phase and finally result after segmentation and the cell analysis: with marked apoptosis (red), the continuum of cell-death morphologies (blue) and necrosis (green).

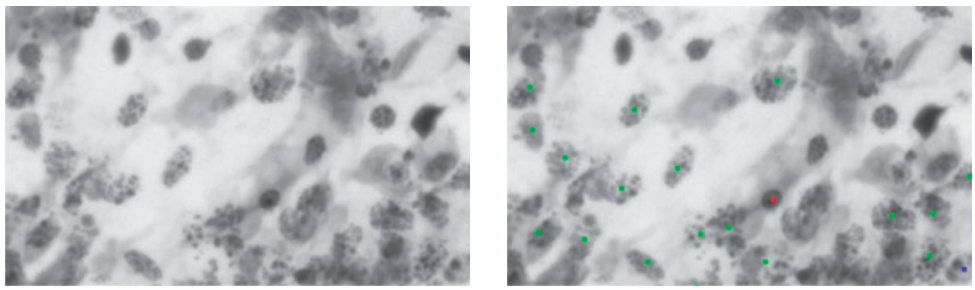

FIGURE 15. Left: Input: original data. Right: Output: data after the segmentation.

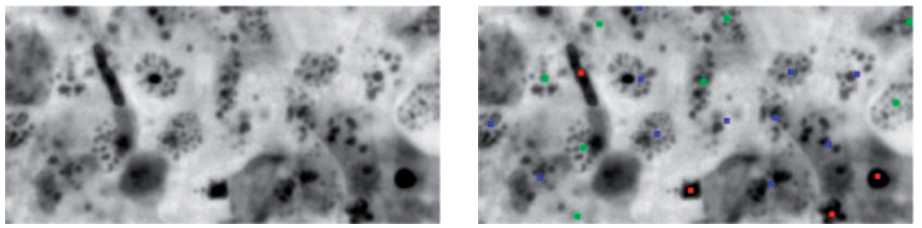

FIGURE 16. Computers detection of the apoptosis, the necrosis and the continuum of cell-death morphologies. Data before and after the processing with the computer software.

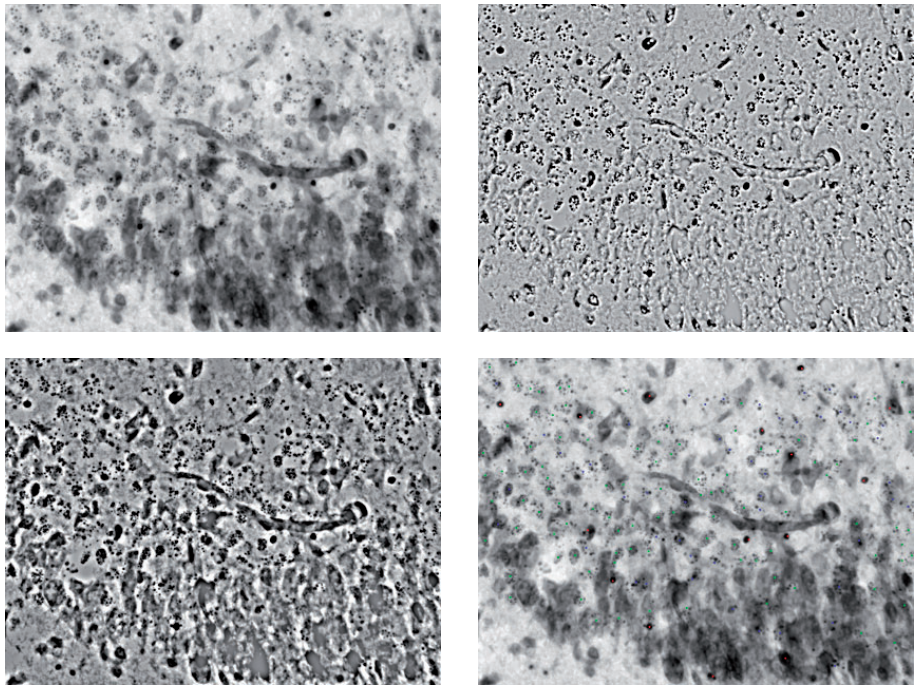

FIGURE 17. Different sample: Before, during pre-processing and after the processing with the computer software.

8. Conclusion and remarks

As the application of the image segmentation approach on the cell categorization problem is in its very beginning phase, a lot of the improvements still need to be done. The score of the cell categories marked automatically correctly without any additional adjustment is between 70 and 85.

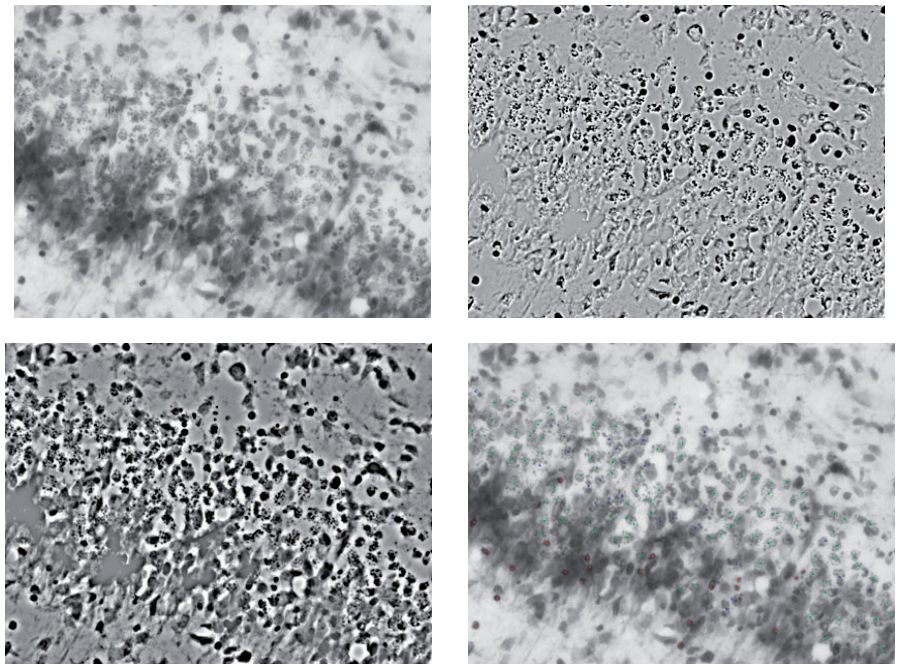

FIGURE 18. Different sample of computer detection of the apoptosis, the necrosis and the continuum of cell-death morphologies. Data before, during pre-processing and after the processing with the computer software.

Nowadays, for more straightforward data, more complex data and global segmentation in tens of seconds and local segmentation of more complex data, it is also real-time. Segmentation speed also depends on the quality of the input data, the dimensions of the image, the selection and the number of seed pixels. The program currently segments either the entire image (globally) or only part of it (locally), depending on what option the user chooses. In the future, it will also be possible to segment the colour images and we would also like to program some other parts so that it would be entirely understandable and clear to the average user. Of course, further optimization of the program is also one of the goals.

Our approach in the detection of apoptosis works with classically stained histological preparations but can also be used for immunofluorescence staining (e.g., DRAQ5TM abcam) to facilitate an image pre-treatment and virtually direct the detection of individual stages of cell death. The procedure of detecting apoptosis based on the morphometric analysis of the set of morphological features has its advantages. Yuncheng et al. [22] used this approach. Their procedure is based on the analysis of three components of image information. Mean values of pixel

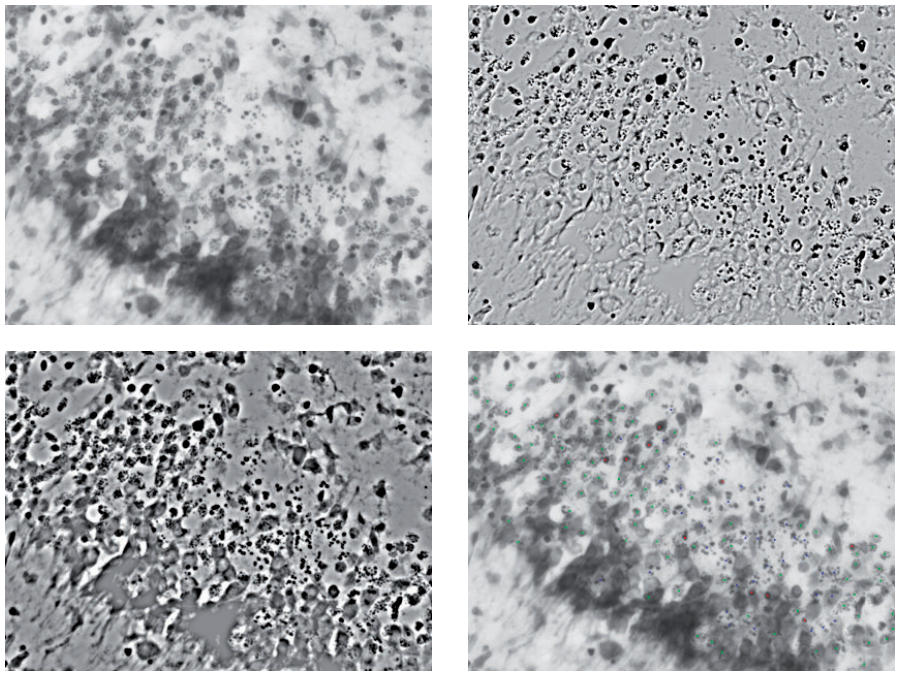

FIGURE 19. Different sample: computer detection of the apoptosis, the necrosis and the continuum of cell-death morphologies.

intensity in cellular areas, deviation of pixel intensity near boundaries and cell border size measurements.

There is a large heterogeneity in the response of individual cells to apoptotic stimuli (Vorobjev and Barteneva [26]). One of the advantages of mathematical procedures for morphometric detection of apoptosis, eventually specially developed programs for this purpose (as in our case), is the flexibility in setting the evaluated parameters. Thus, it is possible for the program "to learn" how to evaluate the occurrence of apoptosis in the cell cultures / histological sections correctly and quickly. Each of the approaches for detecting apoptosis has its advantages but also its disadvantages.

Relatively accurate flow cytometric measurements provide good results but, on the other hand, it does not consider the dynamics of cell death. Therefore, we cannot capture the presence of secondary necrotic cells that have undergone the apoptotic phase. Here we would see the advantage of morphological procedures when analysing time slice images of cell cultures detected by the differential phase contrast method or fluorescent labelled cells.

Note: The preliminary version of this paper was presented as [24].

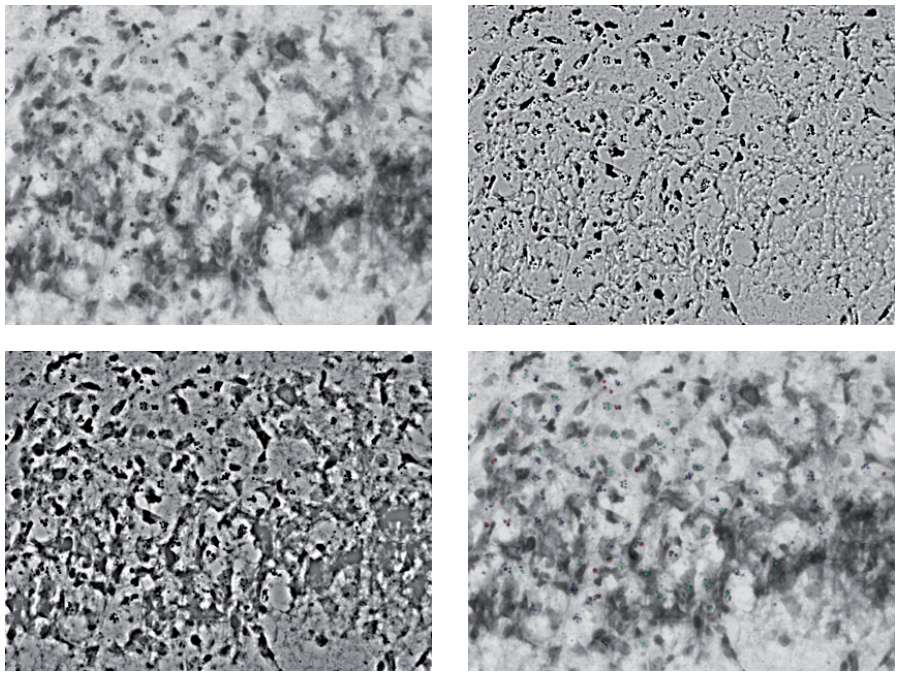

FIGURE 20. Different sample: computer detection of the apoptosis, the necrosis and the continuum of cell-death morphologies. Data before, during pre-processing and after the processing with the computer software.

REFERENCES

[1] BASAVAPRASAD, B.—HEGADI RAVIDRA, S.: *A survey on traditional and graph theoretical techniques for image segmentation*, Internat. J. Comput. Appl. (0975–8887), Recent Advances in Information Technology **1** (2014), 38–46.

[2] BOYKOV, Y.—JOLLY, M. P.: *Interactive graph cuts for optimal boundary and region segmentation of objects in N-D images*, In: Proceedings of International Conference on Computer Vision, Vancouer, Canada, 2001, pp. 105–112.

[3] BONDY, J. A.—MURTY, U. S.: *Graph Theory with Applications*, Great Britain, The Macmillan Press L.t.d, 1976.

[4] CARPENTER, A.—JONES, T.—LAMPRECHT, M. ET ALL: *Cell Profiler: image analysis software for identifying and quantifying cell phenotypes*, Genome Biol. **7** (2006), 1–11.

[5] COHEN, M.—SUM, G.—SNOWDEN R.—DENSDALE D.— SKILLETER, D.: *Key morphological features of apoptosis may occur in the absence of internucleosomal DNA degradation*, Biochem Journal **286** (1991), 331–334.

[6] ECGEVERRI, C. J.—PERRIMON, N.: *High-throughput RNAi screening in cultured cells: A user's guide*, Nat. Rev. Genet. **7** (2006), 373–384.

[7] EGGERT, U. S.—MITCHINSIN, T. J.: *Small molecule screening by imaging*, Curr Opin Chem Biol **10**, (2006), 232–237.

[8] FORD, J. R., L. R.— FULKERSON D. R.: *Maximal flow through a network*, Canadian Journal of Mathematics **8**, (1956), 399–404.

[9] FORD, J. R., L. R.— FULKERSON D. R.: *Flows in Networks*. Princeton University Press, Princeton, New Jersey 1962.

[10] FECKOVÁ-ŠKRABUĽÁKOVÁ, E.—GREVŠOVÁ: *Costs saviing via graph colouring problem approach*, Scientific papers of the university of Pardubice: Series D, **45** (2019), no. 1, 152–160.

[11] GOLDBERG, A. V.—TARJAJN R. E.: *A new approach to the maximum flow problem*, J. Assoc. Comput. Machinery **35**, (1988), 921–940.

[12] GÓMEZ, D.—YANEZ J.—GUADA C.—TINGARUO RODRIGUEAZ J.—MONTERO J.—E. ZARRAZOLA: *Fuzzy image segmentation based upon hierarchical clustering*, Knowledge-Based Systems **87** (2015), 25–37.

[13] KERR, J. F.—WYLLIE, A. H.– CURRIE, A. R.: *Apoptosis: a basic biological phenomenon with wide-ranging implications in tissue kinetics*, Br J. Cancer. **4** (1972), no.4, 239–257.

[14] KOPÁNI, M.—FILON, B.—SEVIK, P.—KRASNAC D.—MISEK, D.—POLAK, S.—KOHAN, M.—MAJOR, J.—ŽDÍMALOVÁ, M.: : *Iron decomposition in rabbit cerebellum after exposure to generated and mobile GSM electromagnetic fields*, Bratislava Medical J. **10** (2017), 575–579.

[15] LINDBLAD, J.—WAHLBY, C.—BENGSTON E.—ZALTSMAN A.: : *Image analysis for automatic segmentation of cytoplasm and classification of Rac1 activation*, Cytometry A **57** (2004), 22–33.

[16] LOUCKÝ, J.—OBERHUBER, T.: *Graph cuts in segmentation of a left ventricle from MRI data*. In: *Proceedings of the Czech–Japanese Seminar in Applied Mathematics 2010*, Czech Technical University in Prague, August 30 - September 4, 2010, pp. 46–54

[17] MURPHY, R. F.—MEIJERING, E.—DANUSER, G.: *Special issue on molecular and cellular bioimaging*, In: *IEEE Transactions on Image Processing*, Vol. 14 (2005), pp. 1233–1236

[18] PERLMAN, Z. E.—SLACK, M. D.—FENG, Y.—MITCHISON, T. J.—WU, L. F.—ALTSCHULER, S. J.: *Multidimensional drug profiling by automated microscopy* Science **306** (2004), no. 5699, 1194–1198.

[19] PENG, B.—ZHANG L.—ZHANG, D.: *A survey of graph theoretical approaches to image segmentation*, Pattern Recognition **46** (2013), 1020–1038.

[20] PRICE, J. H.—GOODACRE A.—HAHN, K. ET ALL.: *Advances in molecular labeling, high throughput imaging and machine intelligence portend powerful functional cellular biochemistry tools*, Journal Cell Biochem. **39** (2002), 194–210.

[21] XIN, J.—RENJ, Z.: *Image Segmentation Based on Level Set Methods*, Physics Procedia **33** (2012), 840–845.

[22] YUCHENG, D.—BUDMAN, H. M.—DUEVER, T. A.: *Segmentation and quantitative analysis of normal and apoptotic cells from fluorescence*, Microscopy Images **49** (2016), 603–608. (IFAC-PapersOnLine)

[23] ŽDÍMALOVÁ, M.—KRIVÁ Z.—BOHUMEL, T.: *Graph cuts in image processing.* In: *14th Conference on Applied Mathematics, APLIMAT 2015*, Institute of Mathematics and Physics, Faculty of Mechanical Engineering, STU in Bratislava, 2015.

[24] ŽDÍMALOVÁ, M.—BOHUMEL, T.—PLACHÁ GREGOROVSKÁ, K.—WESMAN, P.—EL FALOUGY, H.: *Graph cutting in image processing handling with biological data analysis.* In: Information Technology, Systems Research and Computational Physics, (Kulczycki P., Kacprzyk J., Kóczy L.T., Mesiar R., Wisniewski R., eds.) *Advances in Intelligent Systems and Computing*, (2020), Springer-Verlag, Berlin 203–2016. DOI: 10.1007/978-3-030-18058-4_16

[25] ZHOU, X.—CAO X.—PERLMAN Z.—WONG, S. T.: *A computerized cellular imaging system for high content analysis in Monastrol suppressor screens*, Journal Biomed. Inform. **39** (2006), 115–125.

[26] VOROBJEV, I. A.—BARTENEVA, N. S.: *Multi-parametric imaging of cell heterogeneity in apoptosis analysis,* Methods **112** (2017), 105–123.

[27] WYLLIE, A.—BEATHE, G.—HARGREAVES, A.: *Chromatin changes in apoptosis*, Histochem Journal **13** (1981), 681–692.

Received April 8, 2019

Slovak University of Technology
in Bratislava
Radlinského 11
SK–810 05 Bratislava
SLOVAK REPUBLIC

E-mail: zdimalova@math.sk
bohumel@gmail.com

Institute of Experimental Pharmacology and Toxicology
Slovak Academy of Sciences
Sasinkova 2
SK–811 08 Bratislava
SLOVAK REPUBLIC

E-mail: plachakaterina@gmail.com

Institute of Anatomy
Faculty of Medicine
Comenius University
of Bratislava
Sasinkova 2
SK–811 08 Bratislava
SLOVAK REPUBLIC

E-mail: peter.weismann@fmed.uniba.sk
hisham.elfalougy@fmed.uniba.sk